Available online at www.sciencedirect.com
SCIENCE DIRECT®
Journal of Sound and Vibration 292 (2006) 571–582
JOURNAL OF SOUND AND VIBRATION
www.elsevier.com/locate/jsvi

On the use of Pade approximants in the estimation of eigenfrequencies and damping ratios of a vibrating system

Joseph Lardies*

Department of Applied Mechanics R. Chaléat, Institute FEMTO-ST, University of Franche-Comte, CNRS-UMR 6174, 25 000 Besançon, France

Received 16 February 2004; received in revised form 12 July 2005; accepted 9 August 2005
Available online 8 November 2005

Abstract

An approach to estimate eigenfrequencies and damping ratios of a vibrating system, in time domain from output data only, is studied. This approach is based on the interpretation of histograms obtained from the poles of Padé approximants. Using properties of the asymptotic location of poles of Padé approximants to rational functions, different subsets of eigenfrequencies and damping ratios are obtained and their histograms plotted. Numerical and experimental examples are presented.

1. Introduction

Modal parameter identification is used to identify those parameters of the model which describe the dynamic properties of a vibrating system. Classical modal parameter extractions usually require measurements of both: the input force and the resulting response in laboratory conditions. However, for some practical reasons, when operational structures are subjected to random and unmeasured forces such as wind, waves, traffic, shocks, or aerodynamics, modal parameters must be extracted from response-only data. The problem of output-only modal analysis has gained considerable attention in recent years and several different approaches to estimate modal parameters from output-only data have been proposed. They include peak-picking from power spectral density functions, autoregressive moving average models, subspace techniques and wavelet transform [1–10]. Output-only methods offer undeniable advantages: they can be applied without interrupting the structure regular service during the experimental tests; they require no special excitation equipment; it is not necessary to know or measure the excitation. The modal parameters play a relevant role in structural monitoring and inspection. In fact, changes in modal parameters may reflect changes in local mechanical properties due to damaging phenomena underway.

In this paper, a statistically procedure for the estimation of natural frequencies and damping parameters of structural systems under white-noise input is shown. The procedure is based on the computation of Padé

*Tel.: +33 3 81 66 60 57; fax: +33 3 81 66 67 00.
E-mail address: joseph.lardies@univ-fcomte.fr.

0022-460X/$ - see front matter © 2005 Elsevier Ltd. All rights reserved.
doi:10.1016/j.jsv.2005.08.010

approximants to the Z-transform of a noisy data sequence [11–14]. Some theoretical properties of poles of Padé approximants to noisy rational functions are then developed.

The paper is organized as follows. First, a model of a vibrating system and its state space representation are given. The poles of the system are related to covariance matrices and modal parameters are obtained from these poles. Since the order of the state space model, or the number of modes, is unknown, we increase this order. Then, the number of Padé approximants increases, and spurious poles appear. We propose statistical methods to eliminate such spurious modes and to determine the true modes. A numerical example and an experimental test are then presented and the paper is briefly concluded.

2. Modelling a vibrating structure

We consider a structure excited by an unknown white-noise input. Our objective is to determine the modal parameters, from the time response delivered by the output of accelerometers in contact with the structure.

For an n'-degree of freedom vibratory system, the equation of motion can be expressed as

$$M_0\ddot{\xi}(t) + C_0\dot{\xi}(t) + K_0\xi(t) = \eta(t), \tag{1}$$

where M_0, C_0 and K_0 are the system mass, damping and stiffness matrices ($n' \times n'$) respectively; $\ddot{\xi}(t)$, $\dot{\xi}(t)$ and $\xi(t)$ are ($n' \times 1$) vectors of acceleration, velocity and displacement and $\eta(t)$ the ($n' \times 1$) unmeasured excitation vector, which is a white-noise sequence. A state-space model can be formed in lieu of the model given by Eq. (1) as

$$\dot{x}(t) = \tilde{A}x(t) + \tilde{B}\eta(t), \tag{2}$$

where $x(t)$ is the $n = 2n'$ dimensional state vector:

$$x(t) = \begin{bmatrix} \xi(t) \\ \dot{\xi}(t) \end{bmatrix}$$

and $\tilde{A}$, $\tilde{B}$ are given by

$$\tilde{A} = \begin{bmatrix} 0 & I \\ -M_0^{-1}K_0 & -M_0^{-1}C_0 \end{bmatrix}, \quad \tilde{B} = \begin{bmatrix} 0 \\ M_0^{-1} \end{bmatrix}.$$

The response of the dynamic system is measured by the r output quantities in the output $y(t)$, using accelerometers. An ($r \times 1$) vector output equation, called the observation equation, can be written as [2] $\ddot{\xi}$

$$y(t) = H_a\ddot{\xi}(t) = H_aM_0^{-1}[-K_0\xi(t) - C_0\dot{\xi}(t) + \eta(t)] \quad \text{or} \quad y(t) = Cx(t) + D\eta(t), \tag{3}$$

where H_a is the output influence matrix ($r \times n'$) for acceleration. This matrix specifies which points of the system are observed from accelerometers. C is the ($r \times n'$) output influence matrix for the state vector $x(t)$ given by $C = H_aM_0^{-1}[-K_0 - C_0]$ and D is an ($r \times n'$) direct transmission matrix given by $D = H_aM_0^{-1}$. Eqs. (2) and (3) constitute the continuous time state space model of a dynamical system. After sampling with constant period Δt and transformation of the $2n'$ first-order differential equations (2) and (3) into a discrete time equation, we obtain the following discrete time state-space model, where a process noise due to disturbances and modelling inaccuracies is added [2,4]

$$x_{k+1} = Ax_k + w_k, \tag{4}$$

where x_k represents the discrete unobserved state vector of dimension $n = 2n'$; $A = e^{\tilde{A}\Delta t}$ is the ($n \times n$) discrete time transition matrix; w_k is given by $w_k = \int_0^{\Delta t} e^{\tilde{A}s}\tilde{B}\eta(t-s)\,ds + w'_k$ with w'_k the process noise. The discrete time observation equation with measurement noise is given by

$$y_k = Cx_k + v_k, \tag{5}$$

where $v_k = D\eta_k + v'_k$ and v'_k is the measurement noise.

3. Estimating the system's poles from covariance matrices

For any $i>0$ we have the $(r \times r)$ covariance matrix $R_i = E[y_k \quad y_{k-i}^{\mathrm{T}}] = CA^iPC^{\mathrm{T}}$ with $P = E[x_k \quad x_k^{\mathrm{T}}]$, where E denotes the expected value operator. It is well known that there exists a set of scalars $a_0, a_1, \ldots, a_{n-1}$, such that [2,7]

$$A^n = a_0 I + a_1 A + \cdots + a_{n-1} A^{n-1}. \tag{6}$$

Substituting Eq. (6) into R_i for $i = n+1, n+2, \ldots, 2n$ we get a set of equations:

$$\begin{aligned} R_{n+1} &= a_0 R_1 + a_1 R_2 + \cdots + a_{n-1} R_n, \\ R_{n+2} &= a_0 R_2 + a_1 R_3 + \cdots + a_{n-1} R_{n+1}, \\ &\vdots \\ R_{2n} &= a_0 R_n + a_1 R_{n+1} + \cdots + a_{n-1} R_{2n-1} \end{aligned} \tag{7}$$

or in matrix form $H(n)a(n) = h(n)$ where $H(n)$, $a(n)$ and $h(n)$ are, respectively, matrices $(rn \times rn)$, $(rn \times r)$ and $(rn \times r)$:

$$H(n) = \begin{bmatrix} R_1 & R_2 & . & R_n \\ R_2 & R_3 & . & R_{n+1} \\ . & . & . & . \\ R_n & R_{n+1} & . & R_{2n-1} \end{bmatrix}, \quad a(n) = \begin{bmatrix} a_0 I_r \\ a_1 I_r \\ . \\ a_{n-1} I_r \end{bmatrix}, \quad h(n) = \begin{bmatrix} R_{n+1} \\ R_{n+2} \\ . \\ R_{2n} \end{bmatrix}.$$

Let us denote the ith column of $H(n)$ by r_i. We get the linear system

$$\chi a = \gamma, \tag{8}$$

where χ, a and γ are matrices $(nr^2 \times n)$, $(n \times 1)$ and $(nr^2 \times 1)$ given by

$$\chi = \begin{bmatrix} r_1 & r_{1+r} & . & r_{1+(n-1)r} \\ r_2 & r_{2+r} & . & r_{2+(n-1)r} \\ . & . & . & . \\ r_r & r_{2r} & . & r_{nr} \end{bmatrix}, \quad a = \begin{bmatrix} a_0 \\ a_1 \\ . \\ a_{n-1} \end{bmatrix}, \quad \gamma = \begin{bmatrix} r_{1+nr} \\ r_{2+nr} \\ . \\ r_{r+nr} \end{bmatrix}.$$

The values $a_0, a_1, \ldots, a_{n-1}$ are obtained as the least-squares solution of Eq. (8) and the system's poles are estimated as the roots of the characteristic polynomial [7]

$$\mu^n = a_0 + a_1 \mu + \cdots + a_{n-1} \mu^{n-1} \tag{9}$$

and are pairwise conjugate. It follows from the consistency of the values a_j and the continuity of the roots of a polynomial, as functions of its coefficients, that the roots of Eq. (9) are consistent estimates of the system's poles. The natural eigenfrequencies f_j and damping ratios ζ_j of the vibrating system are then given by [3]

$$\lambda_j = \log(\mu_j)/\Delta t, \quad f_j = |\lambda_j|/2\pi, \quad \zeta_j = -\mathrm{Re}(\lambda_j)/|\lambda_j| \quad \text{with } j = 1, \ldots, n'.$$

Only a sequence of observations $\{y_k\}$ is measured and known. The order n of the system or equivalently the number of modes n' in a frequency band of the vibrating system is unknown. Our objective is to increase progressively n, to form χ and γ and to obtain a by resolution of Eq. (8). The system's poles are then estimated by solving the characteristic polynomial. However if n increases, spurious poles or spurious modes appear and our objective is to differentiate these spurious poles or spurious modes from real modes of the vibrating system. The idea is the following. It is well known that to apply the characteristic polynomial method is equivalent to compute the Padé approximants to the Z-transform of the theoretically "infinite" data sequence $\{y_k\}$. More specifically, the poles of the $[n-1, n]$ Padé approximants are the roots μ_j of the characteristic polynomial. Therefore, studying the locus of the poles of the Padé approximants gives information about the location of μ_j. The basic mathematical tool is provided by a theorem due to Gammel and Nuttall [12] in the

framework of the theory of convergence of the Padé approximants, from which it follows that a subset of the poles of the considered Padé approximants converges asymptotically to μ_j.

4. Padé approximants

An accelerometer output is modelled as $y_k = s_k + n_k$ where s_k is the signal noiseless and n_k denotes the measurement noise. The n_k are independent and identically distributed random variables with zero mean. Let $f(z)$ denote the Z-transform of the sequence $\{y_k\}$ defined by the Laurent power series

$$f(z) = \sum_{k=0}^{\infty} y_k z^{-k}. \tag{10}$$

From the coefficients in this power series we may compute the rational Padé approximants to the function $f(z)$. The Padé approximant $f_{m,n}(z)$ of orders m and n to $f(z)$ is a rational function defined by [11–14]

$$f_{m,n}(z) = P_1(z^{-1})/P_2(z^{-1}). \tag{11}$$

We can write $f(z)$ as

$$f(z) = \sum_{k=0}^{\infty} s_k z^{-k} + \sum_{k=0}^{\infty} n_k z^{-k} = s(z) + n(z), \tag{12}$$

where the first term is given by the rational function

$$s(z) = \sum_{j=1}^{n} \frac{c_j}{1 - z_j z^{-1}}. \tag{13}$$

The z_j are the poles of $s(z)$ and are equal to the roots μ_j of the characteristic polynomial, under the assumption of moderate noise. Indeed, if the noise is moderate, computational experiments and Gammel and Nuttall [12] show that the Padé approximants converge to $s(z)$ inside and outside the unit circle. The asymptotic location of the poles of the Padé approximant $f_{m,n}(z)$ are obtained from the theorem of Gammel and Nuttall [12] and from papers of March and Barone [13,14]. Let C be a contour not intersecting the unit circle. If C surrounds a pole z_j of $s(z)$ and no other poles, the residue of $f(z)$ at the pole z_j is

$$\frac{1}{2\pi \mathrm{i}} \int_C f(z)\,\mathrm{d}z = c_j z_j. \tag{14}$$

If the Padé approximant $f_{m,n}(z)$ has h poles inside C denoted by $z_1^*, \ldots, z_h^*$, the residue of $f_{m,n}(z)$ at the pole z_j^* is $c_j^* z_j^*$ and by using the residue theorem we have

$$R_C = \frac{1}{2\pi \mathrm{i}} \int_C f_{m,n}(z)\,\mathrm{d}z = \sum_{j=1}^{h} c_j^* z_j^*. \tag{15}$$

Denote now by C_δ a closed curve lying inside C such that $\min |z - \hat{z}| < \delta$ with $z \in C$, $\forall \hat{z} \in C_\delta$, $\delta > 0$, and let C be a contour not intersecting the unit circle and $m = q + n$. Then, given $\varepsilon > 0$, $\delta > 0$ and $q \in Z$, there exist an n_0 and a contour C_δ lying inside C such for all $n > n_0$ the following properties hold:

(a) if C surrounds a pole z_j of $s(z)$ and no other poles, the Padé approximant $f_{m,n}(z)$ has at least one pole inside C_δ and $|R_{C_\delta}| > |c_j z_j| - \varepsilon$. Indeed, from the theorem due to Gammel and Nutall [12] we have

$$\left| f(z) - f_{m,n}(z) \right| < \varepsilon, \tag{16}$$

so that $\left| f(z) - f_{q+n,n}(z) \right| < 2\pi\varepsilon / L_{C_\delta}$ where $z \in C_\delta$ and L_{C_δ} is the length of the contour C_δ.
We obtain then

$$\varepsilon > \frac{1}{2\pi} \int_{C_\delta} |f(z) - f_{q+n,n}(z)|\,|\,\mathrm{d}z|$$

and it follows that

$$\varepsilon > \frac{1}{2\pi}\left|\int_{C_\delta}(f(z)-f_{q+n,n}(z))\,\mathrm{d}z\right|$$

so that

$$\varepsilon > \left|\frac{1}{2\pi\mathrm{i}}\int_{C_\delta} f(z)\,\mathrm{d}z\right| - \left|\frac{1}{2\pi\mathrm{i}}\int_{C_\delta} f_{q+n,n}(z)\,\mathrm{d}z\right| = |c_j z_j| - |R_{C_\delta}|$$

and we have $|R_{C_\delta}| > |c_j z_j| - \varepsilon$.

(b) if no poles of $s(z)$ lie inside C we have $|R_{C_\delta}| < \varepsilon$. Indeed we have

$$\frac{1}{2\pi\mathrm{i}}\int_{C_\delta} f(z)\,\mathrm{d}z = 0,$$

so that using the theorem due to Gammen and Nuttal

$$|R_{C_\delta}| = \left|\frac{1}{2\pi\mathrm{i}}\int_{C_\delta} f_{q+n,n}(z)\,\mathrm{d}z\right| < \varepsilon.$$

The first property indicates that Padé poles approximate the polar singularities z_j of $s(z)$ inside the unit circle. Hence, if we compute many estimates of the poles $\hat{\mu}_j$ by varying the order n of the system, then for n large enough, the computed Padé poles will give rise to clusters containing spurious poles in the complex plane, around the poles of interest μ_j. However, from the two properties, it follows that the residues of spurious poles can be expected to be much smaller than the residues of the Padé poles. The spurious poles may then be eliminated by looking at the estimated amplitudes of the residues. Numerical and experimental examples show the effectiveness of the procedure in the following section.

5. Application to simulated results

In order to show the usefulness of the Padé approximants theory in modal analysis a simulation is performed with a 3 degrees of freedom system viscously damped. In our simulation we have considered academically the example of a vibrating system represented by masses and springs:

$$M_0 = \begin{bmatrix} 0.13 & 0 & 0; & 0 & 0.2 & 0; & 0 & 0 & 0.15 \end{bmatrix},$$
$$K_0 = \begin{bmatrix} 30 & -10 & 0; & -10 & 15 & -5; & 0 & -5 & 12 \end{bmatrix},$$
$$C_0 = 0.1M_0 + 0.01K_0.$$

All masses are randomly excited with a zero-mean white noise. The number of data points per channel is 1000 and the sampling time is $\Delta t = 0.15$ s. The exact natural frequencies and damping coefficients of the vibrating system are: $f_1 = 0.957$ Hz; $f_2 = 1.564$ Hz; $f_3 = 2.531$ Hz; $\zeta_1 = 0.0384$; $\zeta_2 = 0.0542$; $\zeta_3 = 0.0826$. We then compute the Padé approximants and their poles for $n = 1, 2, \ldots, 40$. The time response of a mass is given in Fig. 1. The poles obtained from Eqs. (8) and (9), using simultaneously three time responses of masses, are plotted in Fig. 2, where the arrows correspond to the true poles. It can be noted that a lot of clusters appear that do not correspond to any of the true poles. The eigenfrequencies histogram is plotted in Fig. 3 before selection. It is very difficult, from this histogram, to determine the true eigenfrequencies of the vibrating system. By interactively choosing a number of classes such that enough resolution is allowed and a threshold, all classes whose values are below the threshold are discarded. To choose the number of classes and a threshold one can plot the power spectral density function of the process and select the frequency intervals where most of the power is concentrated. Then, a value of the number of classes and a threshold are chosen, all the poles in the discarded classes are removed and the histogram of the good poles is computed as shown in Fig. 4. This figure shows the histogram of eigenfrequencies selected. From this figure three frequencies, corresponding to the natural frequencies of the vibrating system, are evident.

The same procedure is applied to determine the true damping coefficients. Figs. 5 and 6 show the histogram of damping coefficients before and after selection. Again three damping coefficients corresponding to the exact

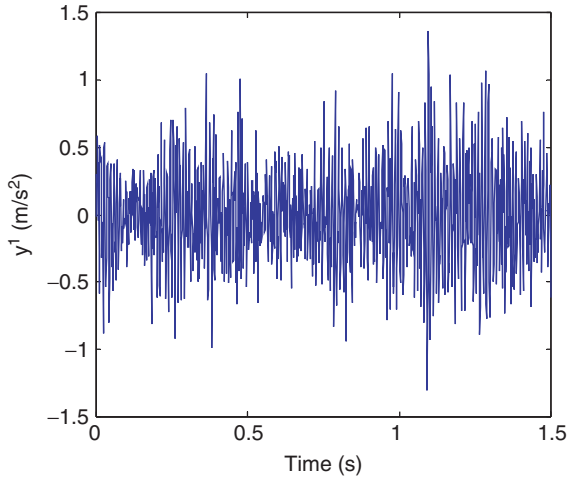

Fig. 1. Acceleration time history for the numerical example.

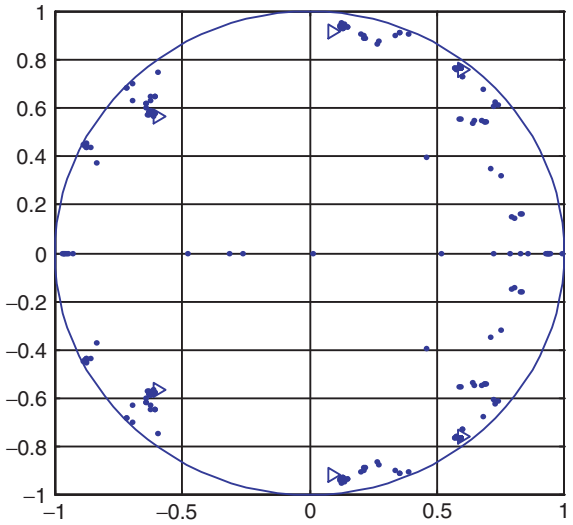

Fig. 2. Computed poles for the numerical example.

damping coefficients of the system are evident in the histogram plotted in Fig. 6. Consider now the case of fairly noisy signals: the simulated data was corrupted by zero mean Gaussian noise. The signal to noise ratio, in terms of rms values, was equal to 10 dB. Figs. 7 and 8 show that the procedure to obtain eigenfrequencies and damping coefficients gives good results with noisy signals. However, if the signal to noise ratio is weak (smaller than 5 dB) the noise affects the results significantly and it is very hard to determine eigenfrequencies and damping ratios. The method failed only in the case of very noisy data (SNR $<$ 5 dB).

6. Application to experimental results

The estimation of eigenfrequencies and damping coefficients is now applied to a mechanical structure of three beams, in laboratory as shown in Figs. 9 and 10. The particularity of this mechanical system is the presence of coupled modes in a frequency band [30–40 Hz]. Three accelerometers are placed on points 1, 3 and 5. Three excitations, which are white-noise, are applied on points 2, 4 and 6. The signals are sampled at rate

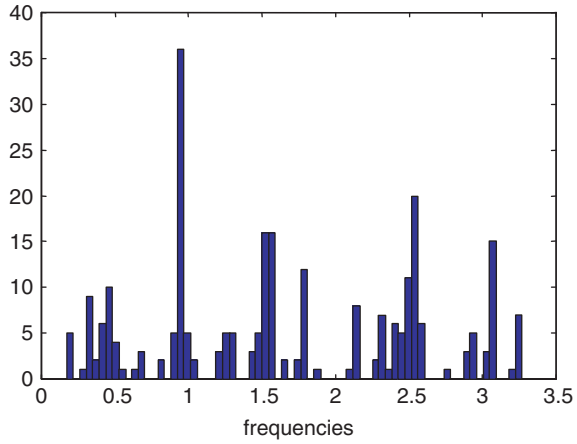

Fig. 3. Histogram of eigenfrequencies before selection for the numerical example.

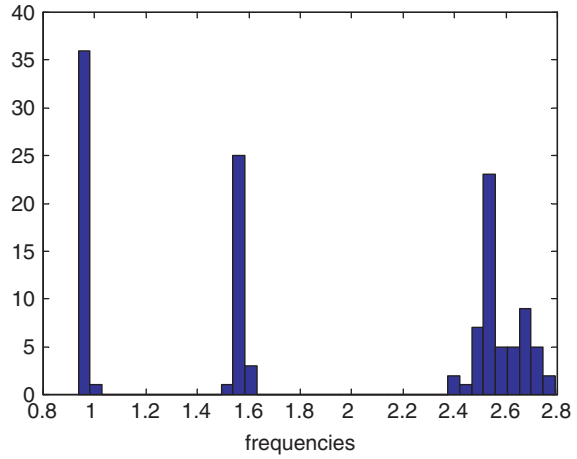

Fig. 4. Histogram of eigenfrequencies after selection for the numerical example.

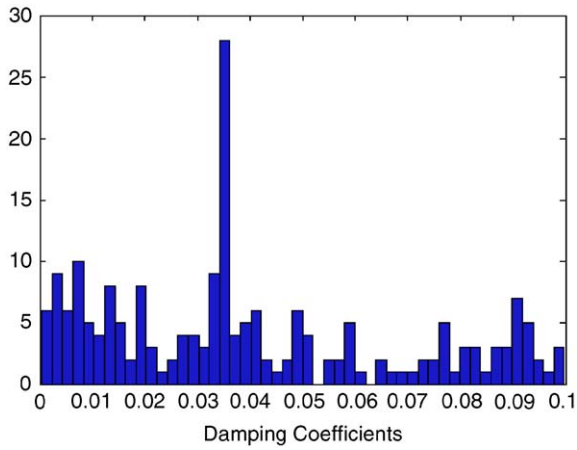

Fig. 5. Histogram of damping coefficients before selection for the numerical example.

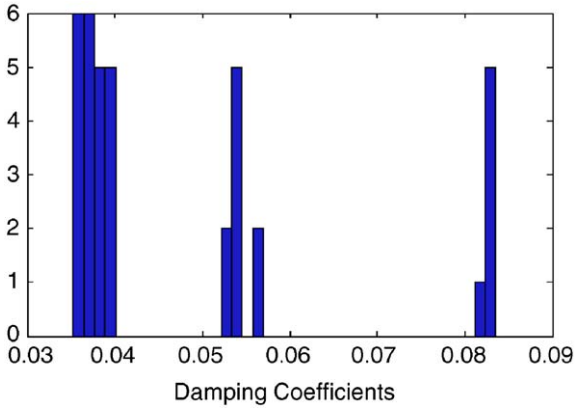

Fig. 6. Histogram of damping coefficients after selection for the numerical example.

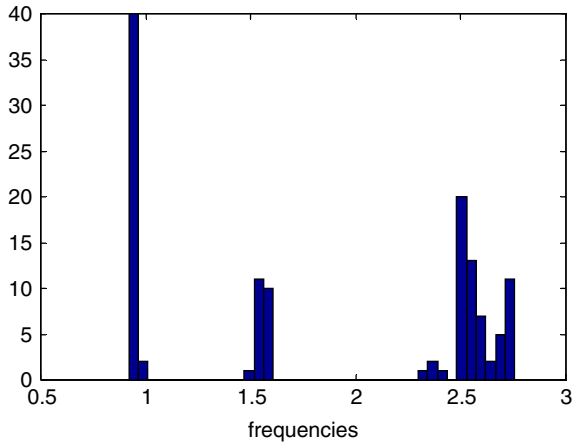

Fig. 7. Histogram of eigenfrequencies after selection for the noisy signal (SNR = 10 dB).

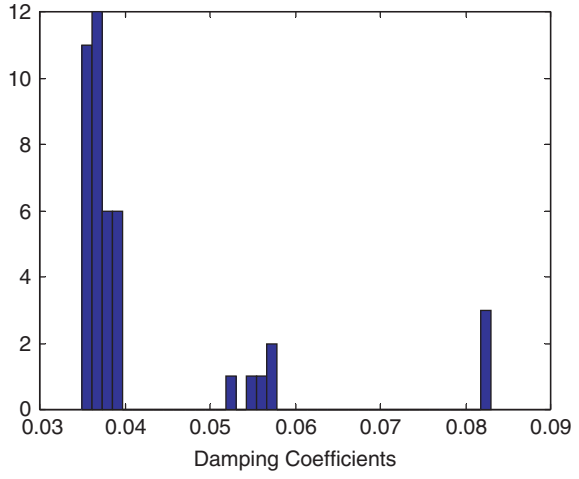

Fig. 8. Histogram of damping coefficients after selection for the noisy signal (SNR = 10 dB).

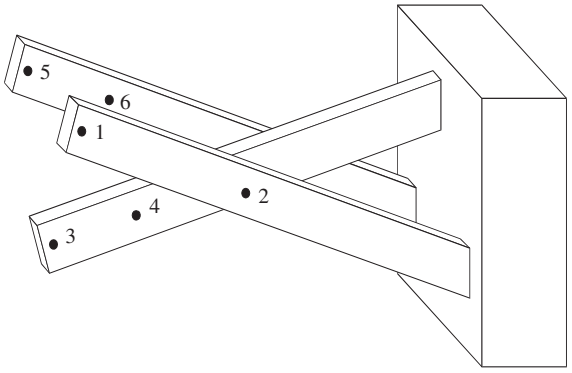

Fig. 9. Plan view of the X-beam.

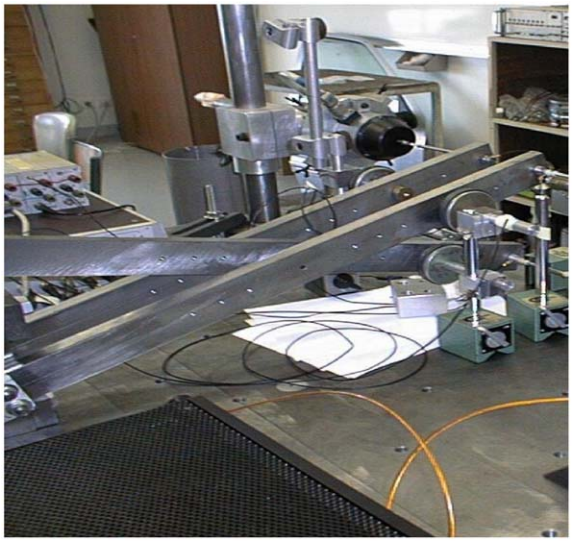

Fig. 10. Experimental X-beam.

$\Delta t = 1.953$ ms and 1500 points are collected for each channel. Fig. 11 shows the time response obtained from one accelerometer. We obtain similar plots if we consider other accelerometers. Figs. 12–14 show the power spectral density response obtained from accelerometers. It is very difficult to extract modal parameters from these plots. Using the time response of all accelerometers and applying the Padé approximation method presented in this paper, the estimated natural frequencies of this mechanical system are $f_1 = 34.3$ Hz, $f_2 = 35.3$ Hz and $f_3 = 36.4$ Hz. They are obtained from the histogram of eigenfrequencies after selection presented in Fig. 15. The corresponding damping coefficients obtained from the histogram plotted in Fig. 16 are $\zeta_1 = 0.0019$; $\zeta_2 = 0.0038$ and $\zeta_3 = 0.0051$.

7. Conclusion

An approach to estimate modal parameters in time domain, from output data only, using Padé approximants associated with a selection procedure of eigenfrequencies and damping coefficients has been presented. Using theoretical properties of the poles of Padé approximants we justify performances of the method. Different histograms of eigenfrequencies and damping coefficients are plotted with a threshold to determine the modal parameters of vibrating systems. This method is very suitable for the analysis of

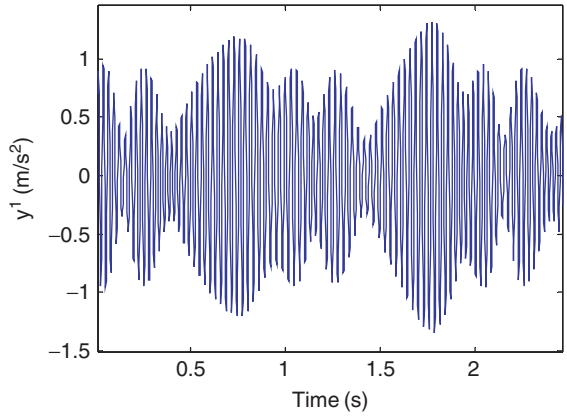

Fig. 11. Acceleration time history from one accelerometer of the X-beam.

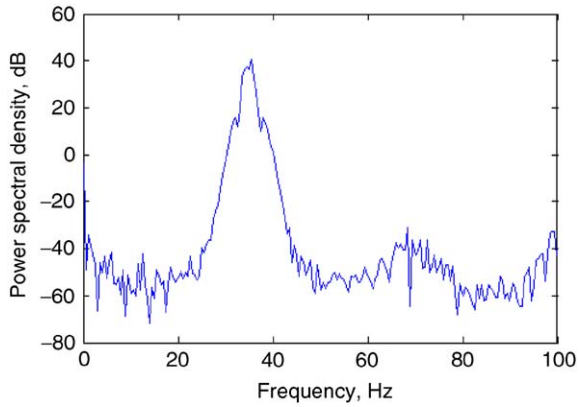

Fig. 12. Frequency response from first accelerometer.

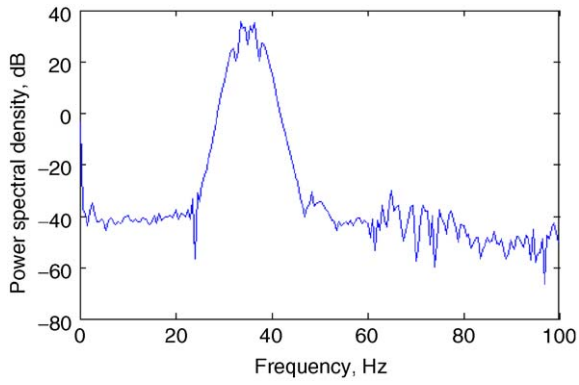

Fig. 13. Frequency response from second accelerometer.

mechanical systems excited by white-noise and has been applied to simulated and real data, obtained from a mechanical system in laboratory. The results obtained underline the accuracy of the procedure in estimating both natural frequencies and damping ratios, whose identification is always critical. The procedure presented is relatively simple but is seen as complementing rather than replacing exiting techniques. However, some problems are still open such as a statistical representation of the effect of the noise on the Padé approximation

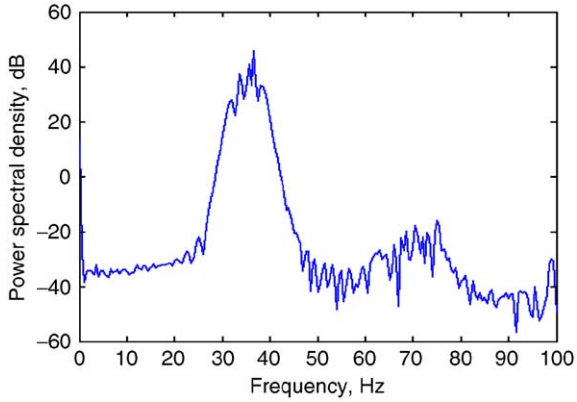

Fig. 14. Frequency response from third accelerometer.

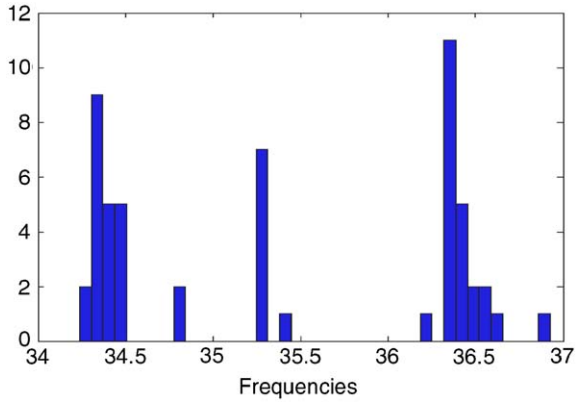

Fig. 15. Histogram of eigenfrequencies after selection for the X-beam.

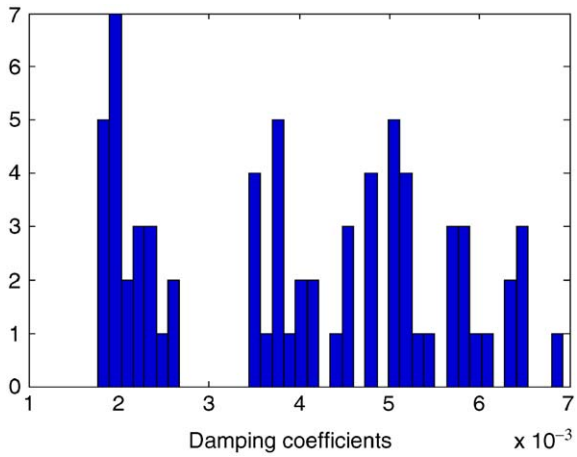

Fig. 16. Histogram of damping coefficients after selection for the X-beam.

process and the quantification of the quality of the results. More studies involving simulated, experimental and industrial systems are required to fully establish the method in particular in the determination of damping coefficients.

References

[1] S.R. Ibrahim, E.C. Mikulcik, A method for the direct identification of vibration parameters from the free response, *Shock and Vibration Bulletin* 47 (Part 4) (1977).
[2] J.N. Juang, *Applied System Identification*, Prentice-Hall, Englewood Cliffs, NJ, 1994.
[3] S. Hu, Y.B. Chen, S.M. Wu, Multi-output modal parameter identification by vector time series modelling, *Twelfth Biennial Conference on Mechanical Vibration and Noise*, New York, 1989, pp. 259–265.
[4] J. lardies, N. Larbi, Modal parameter estimation: an approach using cumulants, *Mechanical Systems and Signal Processing* 17 (2) (2003) 433–442.
[5] C.S. Li, W.J. Ko, H.T. Lin, R.J. Shyu, Vector autoregressive modal analysis with application to ship structures, *Journal of Sound and Vibration* 167 (1) (1993) 1–15.
[6] C.S. Huang, Structural identification from ambient vibration measurement using the multivariate AR model, *Journal of Sound and Vibration* 241 (3) (2001) 337–359.
[7] Y. Baram, Recovering the poles of linear systems, *IEEE Transactions on Automatic Control* 27 (6) (1982) 1157–1160.
[8] M.Q. Feng, J.M. Kim, H. Xue, Identification of a dynamic system using ambient vibration measurements, *Journal of Applied Mechanics* 65 (4) (1998) 1010–1021.
[9] M. Ruzzene, A. Fasana, L. Garibaldi, B. Piombo, Natural frequencies and dampings identification using wavelet transform: application to real data, *Mechanical Systems and Signal Processing* 11 (2) (1997) 207–218.
[10] C.H. lamarque, S. Pernot, A. Cuer, Damping identification in multi-degree of freedom systems via a wavelet logarithmic decrement—part 1: Theory, *Journal of Sound and Vibration* 235 (3) (2000) 361–374.
[11] P.R. Graves-Morris, *Padé Approximants and Their Functions*, Academic Press, New York, 1973.
[12] J. Nuttall, J.L. Gammel, Convergence of Padé approximants to quasianalytic functions beyond natural boundaries, *Journal of Mathematical Analysis and Applications* 43 (1973) 694–696.
[13] P. Barone, R. March, Some properties of the asymptotic location of Padé approximants, *IEEE Transactions on Signal Processing* 46 (9) (1998) 2448–2457.
[14] R. March, P. Barone, Application of the Padé method to solving the noisy trigonometric moment problem, *SIAM Journal of Applied Mathematics* 58 (1) (1998) 324–343.